PROCEEDINGS OF SCIENCE

Lattice $B \to D^{(*)}$ form factors, $R(D^{(*)})$, and $|V_{cb}|$

Andrew Lytle*
INFN, Sezione di Roma Tor Vergata, Via della Ricerca Scientifica 1, 00133 Roma RM, Italy
E-mail: andrew.lytle@roma2.infn.it

I discuss recent progress in lattice calculations of $B \to D^{(*)}\ell\nu$ form factors, important for the precision determination of $|V_{cb}|$ in the Standard Model (SM), and for testing SM expectations of lepton flavor universality in observables $R(D^{(*)})$. I also discuss progress in calculations of the related $b \to c$ semileptonic decays $B_s \to D_s^{(*)}\ell\nu$ and $B_c \to J/\psi\,\ell\nu$ now experimentally accessible at the LHC.

The 37th Annual International Symposium on Lattice Field Theory - LATTICE2019
16-22 June, 2019
Wuhan, China.

*Speaker.

PoS(LATTICE2019)228

1. Introduction

The B-meson semileptonic decays $B \to D^{(*)} l\nu$ provide a precise way to determine the CKM matrix element $|V_{cb}|$. In addition to experimental data, these determinations require the precision calculation of nonperturbative form factors using lattice QCD. There is a long-standing discrepancy between the values obtained from these exclusive determinations $|V_{cb}|^{\text{excl}}$, and those obtained from inclusive determinations $|V_{cb}|^{\text{incl}}$ – this is known as the V_{cb} puzzle [1]. A recent comparison of inclusive and exclusive determinations of $|V_{cb}|$ from the Flavor Lattice Averaging Group (FLAG) is presented in Fig. 1. [1]

There are also long-standing few-sigma discrepancies with Standard Model (SM) predictions in the measured 'R-ratios' for these decays. The R-ratio for a semileptonic decay is defined as the branching fraction for that decay into the tau channel divided by that for the muon or electron,

$$R(D^{(*)}) = \frac{\mathscr{B}(B \to D^{(*)}\tau\nu_\tau)}{\mathscr{B}(B \to D^{(*)} l\nu_l)} \qquad l = \mu, e\,. \tag{1.1}$$

These ratios are independent of $|V_{cb}|$, but depend on the nonperturbative form factors over the entire kinematic range. Recently a measurement from LHCb found that $R(B_c \to J/\psi)$ also differs significantly from its SM expectation [2]. A recent synopsis of the situation for $R(D^{(*)})$ from the Heavy Flavor Averaging Group (HFLAV) is reproduced in Fig. 2.

At the same time, a great deal of new experimental information is expected to become available in the near future, both at Belle II [3] and from the LHC [4]. This will lead to increasingly precise experimental information for $B \to D^{(*)}$, and information about newly accessible decays at LHC in channels $B_s \to D_s^{(*)}$ [5] and $B_c \to J/\psi$ [2], as well as in baryonic channels [6, 7], and increasingly precise R-ratio determinations (see Fig. 2). Keeping pace with these advances is an important challenge for the lattice community. Therefore now is a good time to take stock of lattice efforts in these directions, and this forms the main goal of the present article.

In the next section I briefly review the theory of semileptonic meson decays relevant for the direct determination of $|V_{cb}|$. The main component of this article is Sec. 3 that attempts to summarise the current status and works in progress on the lattice. Much of this material is new/preliminary and was first presented at this conference. Finally in Sec. 4 I will conclude with a short summary and some considerations for the future.

2. Theory

The Standard Model parameter $|V_{cb}|$ can be extracted precisely using the semileptonic decay processes $B \to D^{(*)} l\nu_l$. In these transitions the initial state b quark is converted to a c quark by the weak interaction current, with an accompanying factor of V_{cb} in the amplitude. In the Standard Model then the differential partial widths for these decays are represented as follows:

$$\frac{d\Gamma}{dw}(B \to D) = (\text{known})|V_{cb}|^2(w^2-1)^{3/2}|\mathscr{G}(w)|^2 \tag{2.1}$$

$$\frac{d\Gamma}{dw}(B \to D^*) = (\text{known})|V_{cb}|^2(w^2-1)^{1/2}\chi(w)|\mathscr{F}(w)|^2 \tag{2.2}$$

[1] A review talk summarising the status of the full CKM matrix was given at this conference by Steve Gottlieb [8].

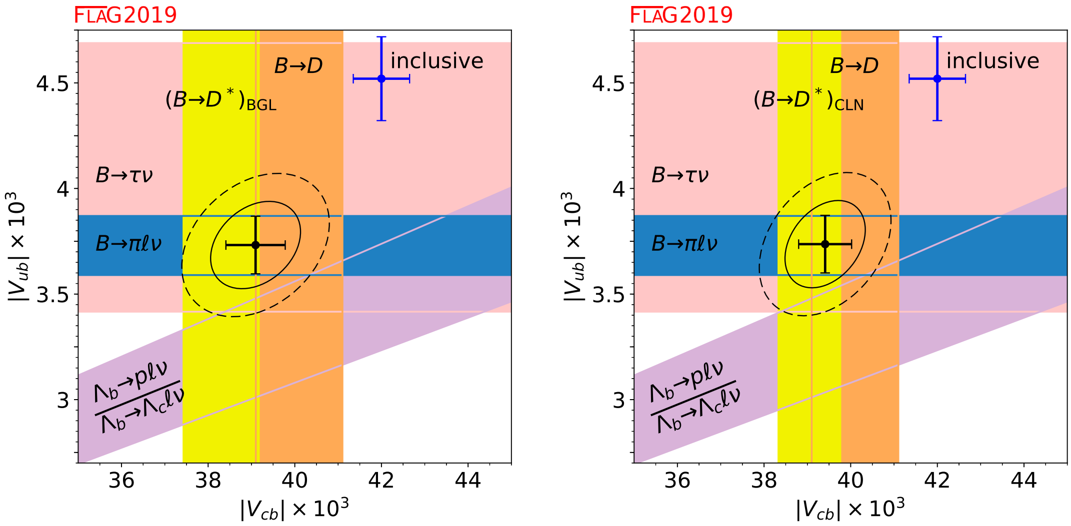

Figure 1: Figures from the 2019 FLAG review [9] showing the present status of $|V_{cb}|$ using various exclusive channels compared with inclusive determinations. The vertical yellow band is the result from $B \to D^* l\nu$ decays using either the BGL (left) or CLN (right) parameterisations to fit the data.

expressed here in terms of the kinematic variable w,

$$w = v_B \cdot v_{D^{(*)}} = \frac{M_B^2 + M_{D^{(*)}}^2 - q^2}{2M_B M_{D^{(*)}}} \tag{2.3}$$

Alternatively the kinematic variable q^2 is often used, where q is the four-momentum transfer between initial and final state mesons. In terms of these variables $q^2 = 0$ corresponds to maximum recoil of the $D^{(*)}$ meson in the B rest frame, while $w = 1$ corresponds to the $D^{(*)}$ at rest in the B rest frame, or $q^2 = q^2_{\rm max} = (M_B - M_D^{(*)})^2$.

In these expressions the non-perturbative QCD dynamics are contained in the functions $\mathscr{F}(w)$ and $\mathscr{G}(w)$. In order to determine $|V_{cb}|$ from the experimental data involving these decays, these functions need to be computed. The functions $\mathscr{F}(w)$ and $\mathscr{G}(w)$ can in turn be expressed in terms of a number of form factors, which are related to the following QCD matrix elements:

$$\frac{\langle D|V^\mu|B\rangle}{\sqrt{m_B m_D}} = (v_B + v_D)^\mu h_+(w) + (v_B - v_D)^\mu h_-(w) \tag{2.4}$$

$$\frac{\langle D^*_\alpha|V^\mu|B\rangle}{\sqrt{m_B m_{D^*}}} = \varepsilon^{\mu\nu\rho\sigma} v_B^\nu v_{D^*}^\rho \varepsilon_\alpha^{*\sigma} h_V(w) \tag{2.5}$$

$$\frac{\langle D^*_\alpha|A^\mu|B\rangle}{\sqrt{m_B m_{D^*}}} = i\varepsilon_\alpha^{*\nu}\left[h_{A_1}(w)(1+w)g^{\mu\nu} - (h_{A_2}(w)v_B^\mu + h_{A_3}(w)v_{D^*}^\mu)v_B^\nu\right] \tag{2.6}$$

These matrix elements can be computed from first principles using the methods of lattice QCD, and from them the form factors determined. In Sec. 3 I will review the state-of-the-art in these calculations, as well as for the related decays involving a $b \to c$ transition but with a strange

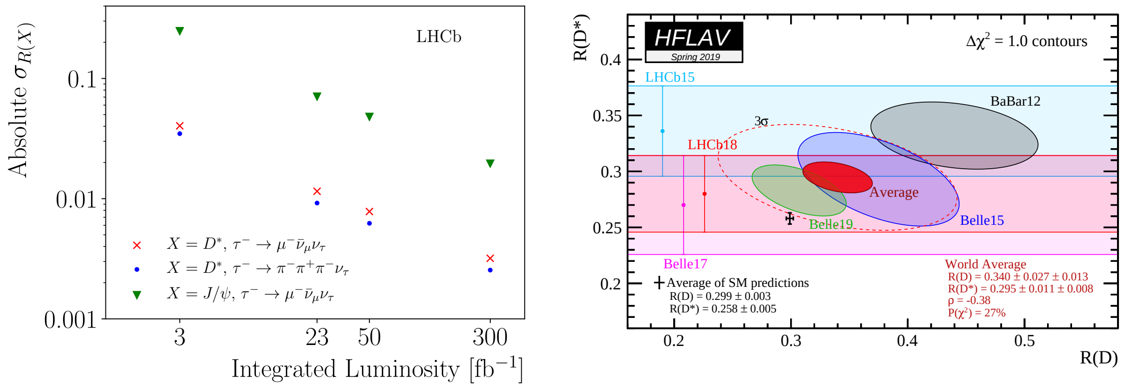

Figure 2: (Left) Projections for the expected uncertainty achievable at LHCb for ratios $R(D^{(*)})$ and $R(J/\psi)$, reproduced from [4]. (Right) Summmary of experimental status of $R(D^{(*)})$ measurements compiled by HFLAV [10].

or charm spectator chark. The formalism described above is analogous for these decays, but the form factors will differ.

In the expressions (2.1), there is a kinematic suppression factor of $(w^2 - 1)$ raised to either the 3/2 or 1/2 power. This results in the experimental rates being damped near $w = 1$, however, as will be discussed in Sec. 3, most available lattice QCD results are limited to the region $w \approx 1$. This is due to the fact that the lattice results are more precise here, their signal decays at larger recoil. In addition, the expressions for the rates (2.1) simplify at the zero-recoil point, so that only a single form factor, $h_{A_1}(1)$ contributes. Therefore the most precise determinations of $|V_{cb}|$ to date have focused on precison lattice calculations of $h_{A_1}(1)$, combined with experimental data in $B \to D^*$, over a range of w which is then extrapolated to $w = 0$.

In recent years some controversy has emerged regarding the precision with which one can reliably extract $|V_{cb}|$ using these extrapolations of the experimental data. In this regard, different methods are now being utilised by both experimental and lattice collaborations. While the Caprini-Lellouch-Neubert (CLN) [11] uses an expansion based on heavy quark effective theory valid to $\mathcal{O}(1/m_{b,c})$, the Boyd-Grinstein-Lebed (BGL) [12] is a model independent parameterisation based on analyticity and unitarity. The CLN approach has the advantage of relying on few parameters, but this restrictiveness may introduce model dependence particularly once a precision beyond the level of approximation is reached [13, 14]. The BGL approach is model independent and as a result relies on more parameters, and must be truncated at some order.

There have been several studies examining the model dependence from different parameterisations in $B \to D$ [13] and $B \to D^*$ [15, 16, 17] decays [18, 19]. This progress was largely facilitated by experimental datasets with q^2 and angular distributions being made publicly available, including full error budgets and correlations [20, 23]. The situation was summarised recently by FLAG [9], reproduced in Fig. 1, showing their best-fits for $|V_{cb}|$ utilising CLN and BGL parameterisations and compared with the inclusive determination.

In order to match experimental data with theory, it is also extremely important for the lattice community to make predictions away from the zero recoil point [1, 18]. Interestingly, in the case of $B \to D$, the picture appears somewhat more congruent than for $B \to D^*$, and here form factors

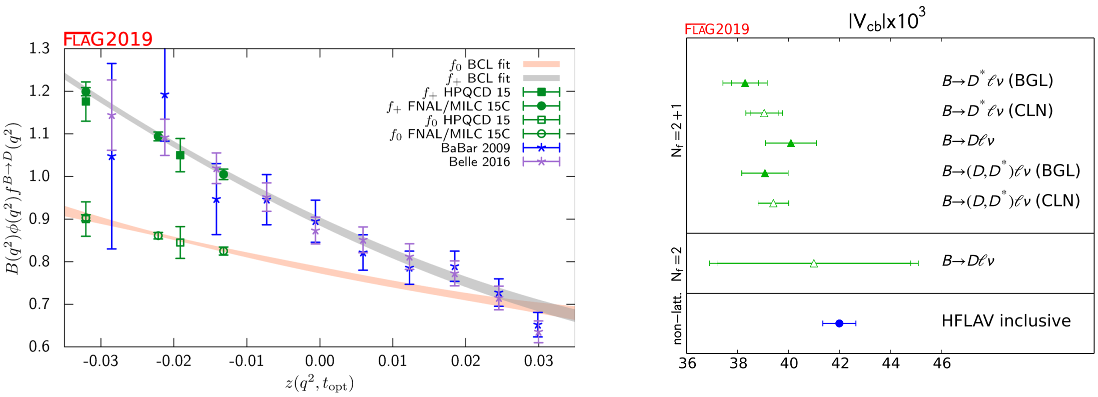

Figure 3: (Left) Comparison of $B \to D$ semileptonic form factors as extracted from experiment (blue, purple) and lattice QCD calculations (green), as summarised in the 2019 FLAG review [9]. (Right) Summary of different $|V_{cb}|$ extractions from FLAG varying the included decay channels and parameterisations used.

are available over a large kinematic range both from experiment [22, 23] and lattice [24, 25]. This is summarised in Fig. 3. Although the final extraction of $|V_{cb}|^{\rm excl}$ from this mode is less precise, it is also in reasonably good agreement with the inclusive determination. With the expected improvements from experiment and the lattice community, as more information becomes available, one imagines that the picture from $B \to D^*$ will become more clear.

It is also interesting to determine the related $B_s \to D_s^{(*)}$ form factors, which differ only in the substitution of the light spectator quark for strange. These decays were recently used by LHCb to measure $|V_{cb}|$ [5]. On the lattice, these calculations should be considerably less computationally expensive due to the reduced cost of strange inversions as compared to light, and also more statistically precise. Therefore it provides both an interesting laboratory in which to test the effect of different parameterizations, as well as make more precision checks between competing lattice determinations. If there are systematic effects impacting a particular calculation of $B \to D^*$, these should show up even more clearly in $B_s \to D_s^*$. Therefore the channels $B_s \to D_s^{(*)}$ should be theoretically pursued.

As will be discussed in Sec. 3, there are now several efforts being undertaken by different groups to extend these calculations beyond zero recoil, as well as explore other $b \to c$ decay modes so that the lattice can be ready for the Belle II and new LHC eras.

3. Lattice QCD results

Here I will briefly summarise the present status of lattice QCD calculations for the group of semileptonic decays $B_{(s)} \to D_{(s)}^{(*)} l\nu$ and $B_c \to J/\psi l\nu$, as well as planned efforts in these directions focusing on preliminary results presented in this conference.

One of the main features that distinguishes amongst these calculations is the choice for the treatment of the b quark in the simulation. Because am_b is not small for the lattice spacings used in many modern simulations, including b in the simulation on the same footing as the other quarks would lead to uncontrollable lattice discretisation errors $\sim (am_b)^n$. Note that the same considera-

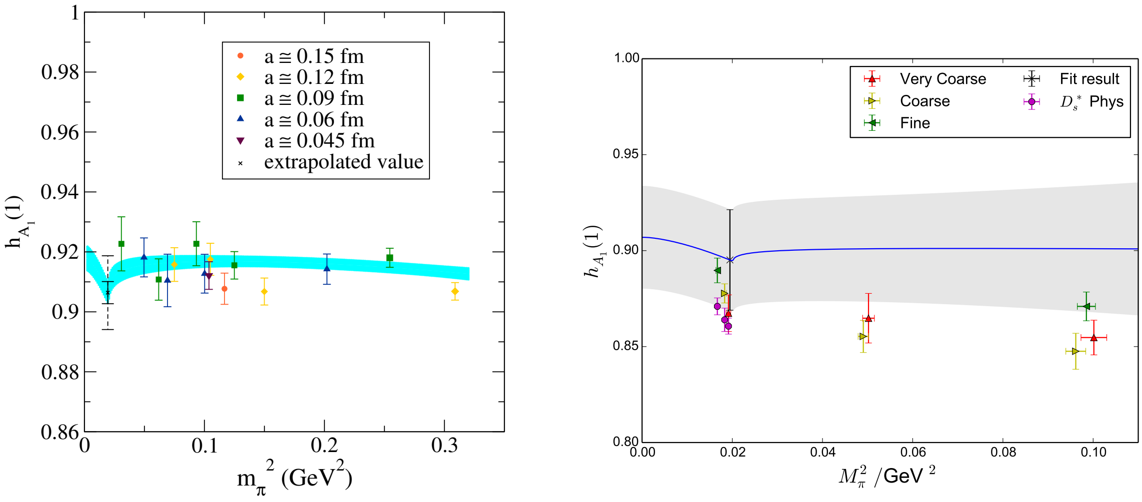

Figure 4: Comparison of chiral-continuum extrapolations for the $B \to D^*$ form factor h_{A_1} at the zero-recoil point, computed by the FNAL-MILC [27] (left) and HPQCD [31] (right) collaborations. The cusp near the physical m_π^2 comes from expectations of chiral perturbation theory.

tions also hold for the charm quark, though it is increasingly common to include it relativistically as lattice spacings decrease. Therefore a strategy such as an effective theory framework must be adopted to incorporate the b quark.

Alternatively, at sufficiently small lattice spacings, it is possible to work at masses m_h approaching m_b such that $am_h \lesssim 1$. By working at several mass values approaching m_b, the lattice data can be extrapolated to a physical prediction at m_b. In what follows I will refer to this as a 'relativistic-b' approach to distinguish it from the effective treatments of b. This method benefits from the use of improved actions which formally improve the form of leading heavy mass discretisation effects, as used in the 'heavy-HISQ' [26] results shown later. A feature of the relativistic-b approach is that it gives not only predictions for the physical decay of a B meson, but also results for masses of the heavy quark between m_c and m_b.

3.1 $B \to D^*$

There are two recent published lattice calculations of the $B \to D^* l\nu$ decay, both at the zero-recoil point, where only the single form factor h_{A_1} contributes. One is from the Fermilab/MILC collaboration, calculated on $n_f = 2+1$ MILC asqtad ensembles, using clover heavy quarks with the Fermilab interpretation [27]. This calculation makes use of the 'ratio-method' [28, 29, 30], wherein they calculate a specific double ratio

$$\frac{\langle D^*|\bar{c}\gamma_j\gamma_5 b|\overline{B}\rangle\langle\overline{B}|\bar{b}\gamma_j\gamma_5 c|D^*\rangle}{\langle D^*|\bar{c}\gamma_4 c|D^*\rangle\langle\overline{B}|\bar{b}\gamma_4 b|\overline{B}\rangle} = |h_{A_1}(1)|^2\,, \tag{3.1}$$

to cancel systematic and statistical errors.

The other is from HPQCD collaboration on $n_f = 2+1+1$ MILC HISQ ensembles, using non-relativistic QCD for the b-quark [31]. The chiral extrapolations for the quantity $h_{A_1}(1)$ are compared in Fig. 4. The two groups find compatible results, quoting $h_{A_1}(1) = 0.906(4)(12)$ and

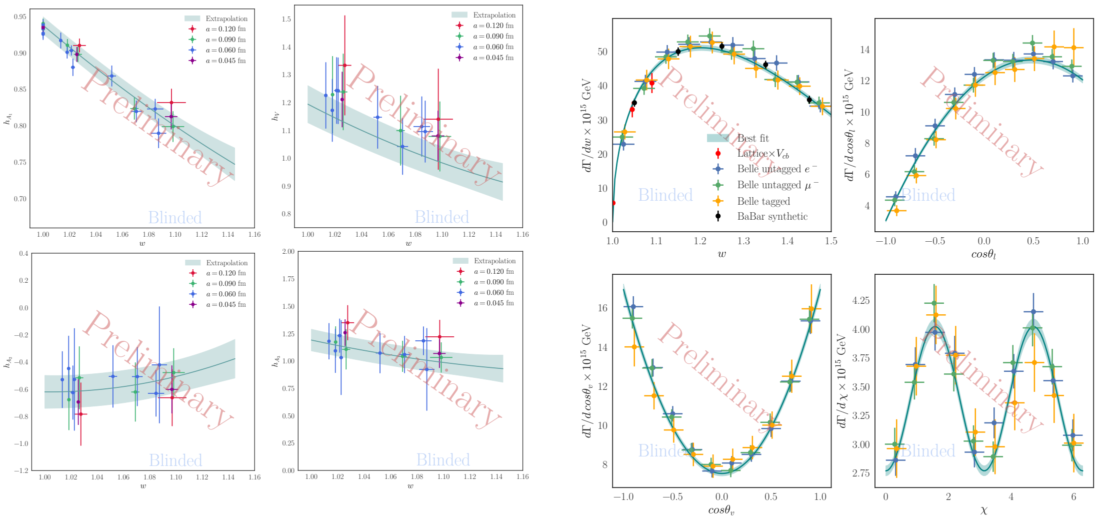

Figure 5: $B \to D^*$ form factors from the MILC collaboration. The figures on the left show the lattice form factors at different values of the lattice spacing and the extrapolated results, the figures on the right show the kinematic distributions derived from a combination fit of lattice and experimental data compared with lattice data and data from Belle and Babar. See also results in [32, 34, 35] Figs. courtesy A. Vaquero.

0.895(10)(24) for FNAL/MILC and HPQCD respectively. The dominant error in [31] arises from missing $\mathscr{O}(\alpha_s^2)$ matching of NRQCD currents to QCD.

The MILC collaboration is extending their calculation to the the full set of form factors, away from zero recoil. Preliminary results in the range $w \in [1, 1.1]$ were presented in [32], and an update was presented at this conference [33] showing global fits and comparison with available experimental data, as shown in Fig. 5.

The JLQCD collaboration have presented their preliminary results for $B \to D^{(*)}$ form factors in [36] for a range $w \in [1, 1.06]$ and at two lattice spacings, and an update of these results were presented at this conference by Kaneko [37], with extended range in $w \in [1, 1.1]$ and including results at a finer lattice spacing of $a^{-1} = 4.5$ GeV. These calculations use a 'relativistic-b' approach on Möbius domain wall fermions, for which observables are calculated over a range of heavy quark masses keeping $am_h < 0.8$, (m_h up to 3.05 m_c), with an extrapolation required to the physical m_b. Their results are shown in Fig. 6 for $h_{A_{1,2,3}}$ and h_V. The extrapolated results for $h_{A_1}(1)$ agree well with FNAL/MILC and HPQCD [27, 31].

The LANL/SWME collaboration have also released preliminary results for the h_{A_1} form factor at zero recoil [38, 39], and at this conference [40]. Their calculation is carried out on the $n_f = 2+1+1$ MILC HISQ ensembles, using the Oktay-Kronfeld (OK) action [41, 42] for valence charm and bottom, at two lattice spacings $a \approx 0.12, 0.09$ fm and a single pion mass $m_\pi \approx 310$ MeV. The OK action is improved at a higher order in $\lambda_{c,b} \sim \frac{\Lambda_{\rm QCD}}{2m_{c,b}}$ than the Fermilab action being used by the MILC collaboration – This is important to reduce the charm quark discretisation error, the dominant (1%) error in [27], to below the percent level [43]. Preliminary results for $h_{A_1}(1)$ are shown in Fig. 7.

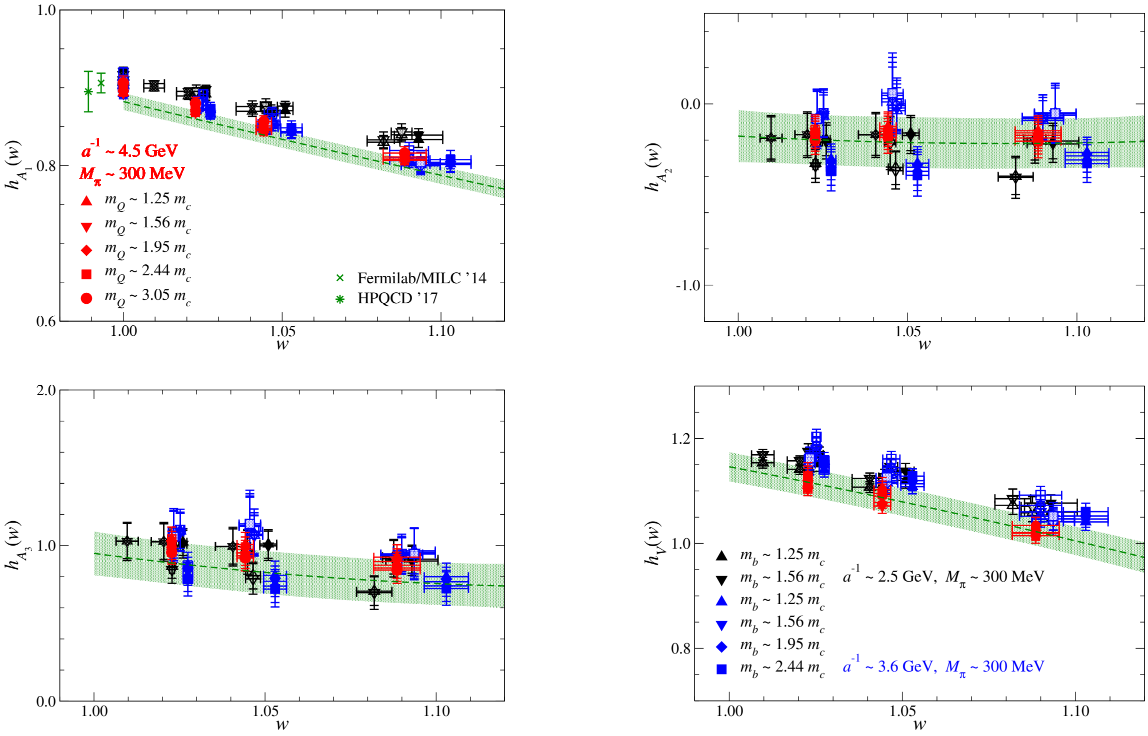

Figure 6: $B \to D^*$ form factors from the JLQCD collaboration, using a 'relativistic-b' approach. New results on a finer $a^{-1} \approx 4.5$ GeV lattice spacing are shown in red, and the result of chiral/continuum extrapolations are shown as green bands. For $h_{A_1}(1)$ the comparison with previous results from [27, 31] are also shown. Figs. courtesy Takashi Kaneko.

3.2 $B \to D$

The FNAL/MILC and HPQCD collaborations have both computed $B \to D$ form factors at zero and non-zero recoil on $n_f = 2+1$ MILC asqtad lattices, the former using heavy quarks in the Fermilab approach [24] and with lattice spacing down to $a \sim 0.045$ fm, the latter using HISQ (relativistic) c and NRQCD b [25] at two lattice spacings of $a \sim 0.09$, 0.12 fm. A comparison of these results reproduced from [9] is shown in Fig. 3 along with experimental data [22, 23]. Their results are in good agreement, although HPQCD has larger errors coming mainly from discretization effects and NRQCD matching uncertainties, similar to the situation for $B \to D^*$.

In contrast to the present situation with $B \to D^*$, here the form factors from lattice are available over an extended range in q^2. After the new lattice data beyond zero-recoil became available as well as new experimental data from Belle, a careful analysis [13] of the available data and different form factor parameterisations found a value for $|V_{cb}| = 40.49(97)10^{-3}$, this value being between, and compatible with, both the inclusive determination and the exclusive value from $B \to D^*$. It is clear from this study the importance of having lattice data away from zero recoil, as well as carefully assessing parameterisation dependence. The lattice and experimental data for the form factors are shown together in Fig. 3.

Preliminary results for $B \to D$ form factors from JLQCD collaboration were presented in [36],

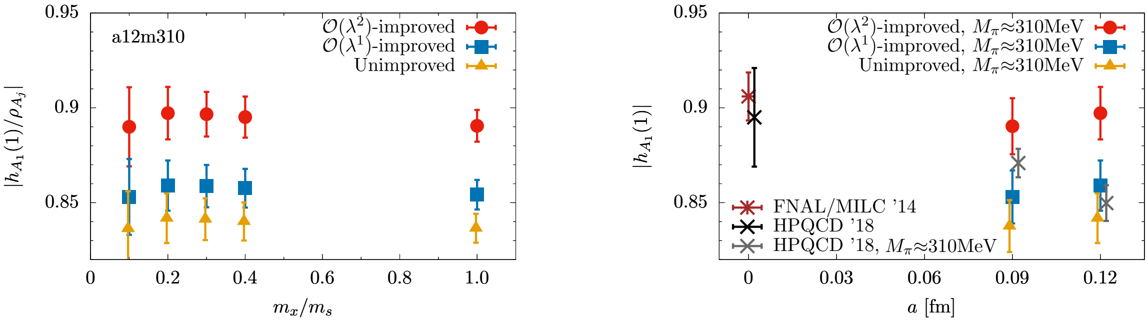

Figure 7: Results for $B \to D^*$ at zero recoil from LANL/SWME [39] showing the effect of higher orders of current improvement (left) and compared with prior results in the literature (right) – Note that ρ_{A_1} is here set to 1 so the comparison is only indicative.

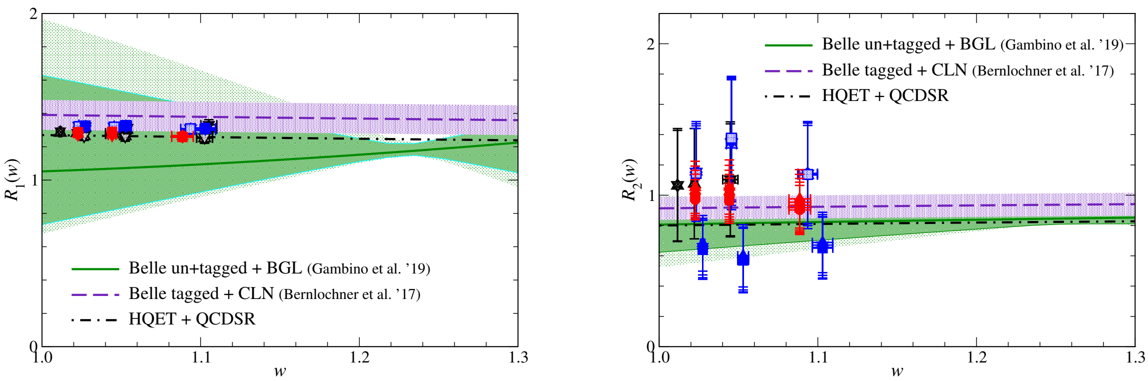

Figure 8: Comparison of lattice form factor data from JLQCD (symbols) with fits to experimental Belle data [20, 21] using different parameterisations (colored bands) [19, 1] and predictions of HQET. For more discussion see [37]. Figs. courtesy Takashi Kaneko.

with an update presented at this conference [37] including lighter pion masses, and a third lattice spacing with $a^{-1} \sim 4.5$ GeV, which allows to extend the heavy quark mass in the simulation to $m_h \sim 3.05 m_c$. RBC/UKQCD also presented [44] preliminary results on $n_f = 2+1$ domain wall ensembles, treating light, strange, and charm quarks with the domain wall action, and the bottom quark with a relativistic heavy quark action as shown in Fig. 9. Preliminary results at two lattice spacings ($a \approx 0.12, 0.09$ fm) and two pion masses ($m_\pi \approx 310$, 220 MeV) were presented by LANL/SWME [40], their results for the $h_{+/-}(w)$ form factors are shown in Fig. 10.

3.3 $B_s \to D_s^*$

There are two determinations of the $B_s \to D_s^*$ zero-recoil form factor $h^s_{A_1}(1)$, both from the HPQCD collaboration using $n_f = 2+1+1$ MILC HISQ ensembles, but differing in the treatment of the b-quark. The calculation of [31] uses an NRQCD b-quark on relatively coarser ensembles, while [45] uses the relativistic 'heavy-HISQ' approach on fine ensembles down to $a \sim 0.45$ fm. The main systematic uncertainty in the NRQCD calculation comes from the perturbative current matching known to $\mathscr{O}(\alpha_s)$, this error is absent from the heavy-HISQ calculation where the current

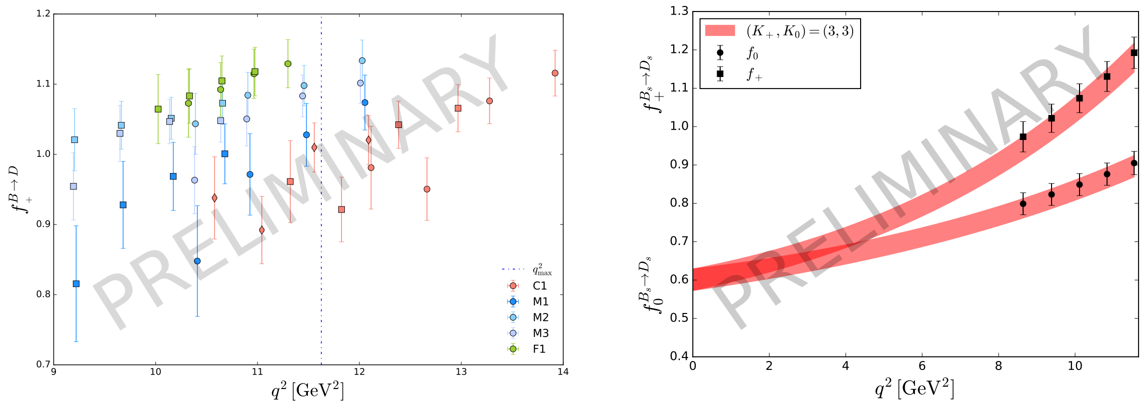

Figure 9: Preliminary results from the RBC/UKQCD collaboration [44]. (Left) Data for $f_+(q^2)$ for $B \to D$ decay. The colors correspond to the different gauge ensembles ($a/L/m_\pi$), and different shapes correspond with different input "charm" masses used to interpolate/extrapolate to physical charm. (Right) The $f_{+/0}(q^2)$ form factors for $B_s \to D_s$ with fits to a CLN parameterization.

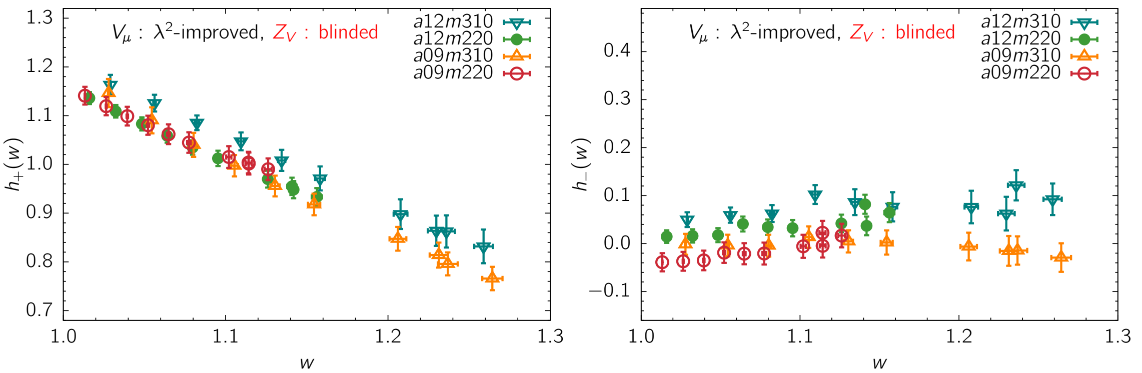

Figure 10: Preliminary results for $B \to D$ $h_+(w)$ (left) and $h_-(w)$ (right) form factors from LANL/SWME [40], at two lattice spacings ($a \approx 0.12, 0.09$ fm) and two pion masses ($m_\pi \approx 310$, 220 MeV). The overall normalisation of the results is blinded.

is normalised non-perturbatively using the PCAC relation. The two calculations are in agreement

$$h^s_{A_1}(1) = 0.883(12)_{\rm stat}(28)_{\rm sys} \tag{3.2}$$

$$h^s_{A_1}(1) = 0.9020(96)_{\rm stat}(90)_{\rm sys} \tag{3.3}$$

It is also interesting to note that in [31] the ratio of zero-recoil form factor with light/strange spectator was calculated to be $h_{A_1}(1)/h^s_{A_1}(1) = 1.013(14)_{\rm stat}(17)_{\rm sys}$. In this ratio the main systematic from the current matching largely cancels.

3.4 $B_s \to D_s$

There have been a few calculations of the $B_s \to D_s$ form factors, using different methodologies. The MILC collaboration determined $f_0(q^2)$ and $f_+(q^2)$ using $n_f = 2+1$ asqtad ensembles, with charm and bottom valence quarks using the clover action with Fermilab interpretation [46, 47]. There was a $n_f = 2$ determination by the ETMC collaboration [48] using twisted Wilson quarks,

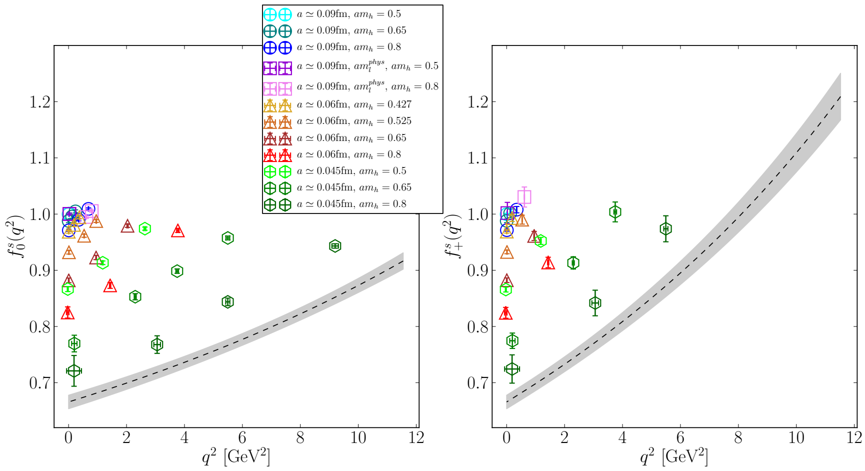

Figure 11: Figure from [51] showing results for $B_s \to D_s$ $f_{0/+}$ form factors using the 'heavy-HISQ' approach. The colored open symbols show raw data for form factors calculated at unphysically light b-quark masses on a range of ensembles with lattice spacings from $a \sim 0.09 - 0.045$ fm. The continuum extrapolated results for the form factors at physical b-quark mass are given by the gray bands.

in which they also determined the ratio of the tensor form factor to f_+ near zero recoil. The RBC/UKQCD collaboration presented preliminary results in [49, 50] and these were updated at this conference [44]. The preliminary results for their form factors are shown in Fig. 9.

Recently the $f_{0/+}$ form factors were computed over the entire kinematic range using the heavy-HISQ approach by the HPQCD collaboration [51]. The raw data at unphysically light b mass and the form factors extrapolated to the b mass are shown in Fig. 11. HPQCD also determined both form factors using NRQCD b in [52]; the results from both calculations are shown in Fig 12.

Until recently the lattice QCD results for $B_s \to D_s^{(*)}$ form factors could not be compared with experiment, that changed with the LHCb measurement [5], resulting in a new determination of $|V_{cb}|$ based on B_s decays. Their analysis was performed using both BGL and CLN parameterizations, and the extracted $|V_{cb}|$ is compatible between the two within errors. Their result is compatible with both inclusive and exclusive determinations from B decays, but with larger errors. These encouraging results increase the urgency for $B_s \to D_s^*$ results away from zero recoil and increasing precision in both channels $B_s \to D_s^{(*)}$.

3.5 $B_c \to J/\psi$

There are currently only preliminary results available for the $B_c \to J/\psi\, l\nu$ lattice form factors [55, 56, 57], by HPQCD using the 'heavy-HISQ' approach. The R-ratio for this decay was measured by LHCb [2], who found $R(J/\psi) = 0.71(17)_{\rm stat}(18)_{\rm syst}$. This value is $\sim 2\sigma$ larger than what is expected in the SM and although this value has large uncertainties it is desirable to have a lattice determination, particularly as the experimental precision improves (see Fig. 2). A preliminary value $R(J/\psi) = 0.2592(92)$ was given in [55], and Fig. 13 shows the differential decay width as a function of q^2.

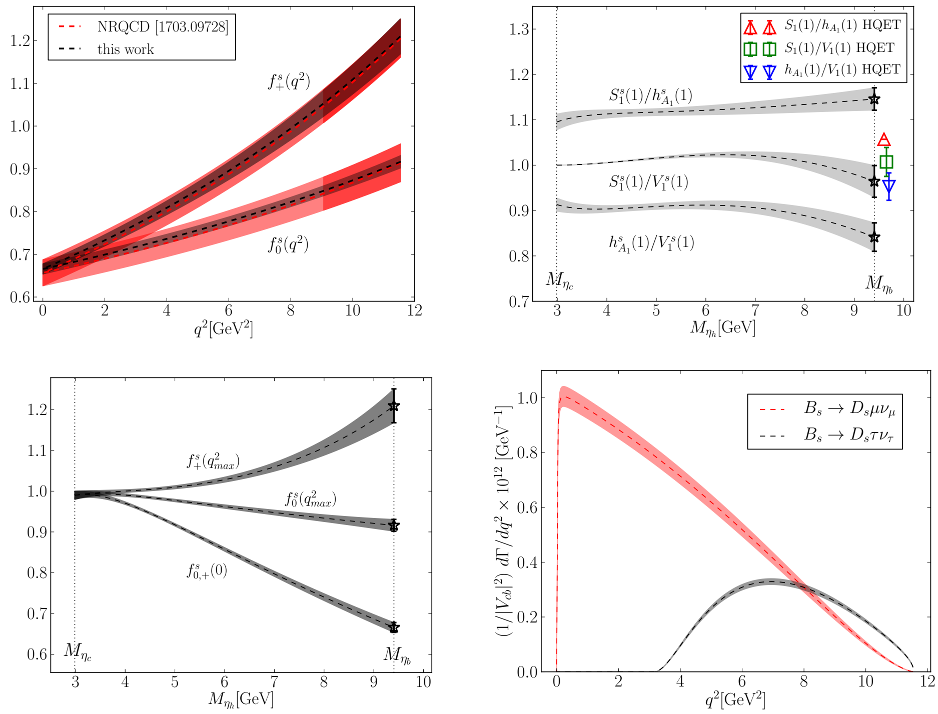

Figure 12: (Top-left) HPQCD's $B_s \to D_s$ form factors $f_{0/+}$ from [51] using the 'heavy-HISQ' approach compared with results from NRQCD [52]. (Top-right) Results for ratios of zero-recoil form factors as a function of M_{η_h} used as a physical proxy for the heavy quark mass m_h used in simulation, compared with predictions of HQET [18]. (Bottom-left) Evolution of the form factor endpoints $f_{0/+}(0, q^2_{\rm max})$ as a function of M_{η_h}. (Bottom-right) Partial differential decays widths for $B_s \to D_s l \nu_l$ for $l = \mu, \tau$.

4. Conclusions

I would hazard that the study of $b \to c$ transitions is at somewhat of a crossroads. There are several long-standing puzzles in this sector where experimental data and theoretical predictions do not quite square, and there are a number of welcome developments on the horizon that will be essential to a precise understanding that can either confirm or rule out these discrepancies. Among these are improved predictions from the lattice community over a larger kinematic range than has heretofore been available, and results in new channels $B_s \to D_s^*$ and $B_c \to J/\psi$, and also in the baryon sector, that can match experimental breakthroughs from LHC. With the imminent results from Belle II, $B \to D^*$ will surely remain the gold standard for extractions of $|V_{cb}|$, and it is therefore a challenge for the lattice community to put these calculations on a solid footing, and in particular away from zero recoil. As reviewed briefly above, fortunately there are several lattice collaborations that have embarked upon this endeavour.

5. Acknowledgements

I would like to thank the organizers of Lattice 2019 for an enjoyable conference and the oppor-

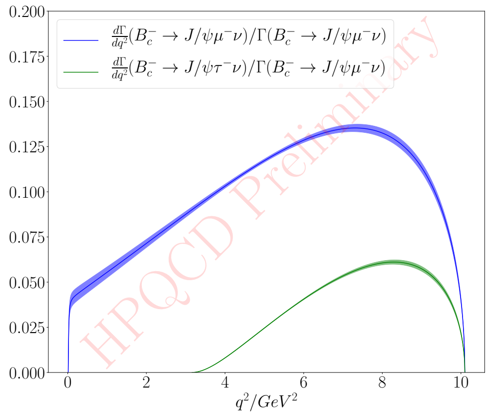

Figure 13: Differential decay widths for $B_c \to J/\psi\, l\nu$ with $l = \mu$ (blue) and $l = \tau$ (green), computed from lattice QCD using the 'heavy-HISQ' methodology. Figure courtesy J. Harrison.

tunity to present this material. I would like to thank C. Davies, G. de Divitiis, B. Dey, J. Harrison, S. Hashimoto, W. Lee, L. Lellouch, S. Meinel, A. Vaquero, and A. Vladikas for useful discussions and insight.

References

[1] P. Gambino, M. Jung and S. Schacht, Phys. Lett. B **795** (2019) 386 doi:10.1016/j.physletb.2019.06.039 [arXiv:1905.08209 [hep-ph]].

[2] R. Aaij *et al.* [LHCb Collaboration], Phys. Rev. Lett. **120** (2018) no.12, 121801 doi:10.1103/PhysRevLett.120.121801 [arXiv:1711.05623 [hep-ex]].

[3] E. Kou *et al.* [Belle-II Collaboration], arXiv:1808.10567 [hep-ex].

[4] R. Aaij *et al.* [LHCb Collaboration], arXiv:1808.08865.

[5] R. Aaij *et al.* [LHCb Collaboration], arXiv:2001.03225 [hep-ex].

[6] R. Aaij *et al.* [LHCb Collaboration], Nature Phys. **11** (2015) 743 doi:10.1038/nphys3415 [arXiv:1504.01568 [hep-ex]].

[7] W. Detmold, C. Lehner and S. Meinel, Phys. Rev. D **92** (2015) no.3, 034503 doi:10.1103/PhysRevD.92.034503 [arXiv:1503.01421 [hep-lat]].

[8] S. Gottlieb, PoS LATTICE **2019** (2019) 275 [arXiv:2002.09013 [hep-lat]].

[9] S. Aoki *et al.* [Flavour Lattice Averaging Group], arXiv:1902.08191 [hep-lat].

[10] Y. S. Amhis *et al.* [HFLAV Collaboration], arXiv:1909.12524 [hep-ex].

[11] I. Caprini, L. Lellouch and M. Neubert, Nucl. Phys. B **530** (1998) 153 doi:10.1016/S0550-3213(98)00350-2 [hep-ph/9712417].

[12] C. G. Boyd, B. Grinstein and R. F. Lebed, Phys. Rev. D **56** (1997) 6895 doi:10.1103/PhysRevD.56.6895 [hep-ph/9705252].

[13] D. Bigi and P. Gambino, Phys. Rev. D **94** (2016) no.9, 094008 doi:10.1103/PhysRevD.94.094008 [arXiv:1606.08030 [hep-ph]].

[14] M. Bordone, M. Jung and D. van Dyk, arXiv:1908.09398 [hep-ph].

[15] D. Bigi, P. Gambino and S. Schacht, Phys. Lett. B **769** (2017) 441 doi:10.1016/j.physletb.2017.04.022 [arXiv:1703.06124 [hep-ph]].

[16] B. Grinstein and A. Kobach, Phys. Lett. B **771** (2017) 359 doi:10.1016/j.physletb.2017.05.078 [arXiv:1703.08170 [hep-ph]].

[17] J. P. Lees *et al.* [BaBar Collaboration], Phys. Rev. Lett. **123** (2019) no.9, 091801 doi:10.1103/PhysRevLett.123.091801 [arXiv:1903.10002 [hep-ex]].

[18] F. U. Bernlochner, Z. Ligeti, M. Papucci and D. J. Robinson, Phys. Rev. D **95** (2017) no.11, 115008 Erratum: [Phys. Rev. D **97** (2018) no.5, 059902] doi:10.1103/PhysRevD.95.115008, 10.1103/PhysRevD.97.059902 [arXiv:1703.05330 [hep-ph]].

[19] F. U. Bernlochner, Z. Ligeti, M. Papucci and D. J. Robinson, Phys. Rev. D **96** (2017) no.9, 091503 doi:10.1103/PhysRevD.96.091503 [arXiv:1708.07134 [hep-ph]].

[20] A. Abdesselam *et al.* [Belle Collaboration], arXiv:1702.01521 [hep-ex].

[21] E. Waheed *et al.* [Belle Collaboration], Phys. Rev. D **100** (2019) no.5, 052007 doi:10.1103/PhysRevD.100.052007 [arXiv:1809.03290 [hep-ex]].

[22] B. Aubert *et al.* [BaBar Collaboration], Phys. Rev. Lett. **104** (2010) 011802 doi:10.1103/PhysRevLett.104.011802 [arXiv:0904.4063 [hep-ex]].

[23] R. Glattauer *et al.* [Belle Collaboration], Phys. Rev. D **93** (2016) no.3, 032006 doi:10.1103/PhysRevD.93.032006 [arXiv:1510.03657 [hep-ex]].

[24] J. A. Bailey *et al.* [MILC Collaboration], Phys. Rev. D **92** (2015) no.3, 034506 doi:10.1103/PhysRevD.92.034506 [arXiv:1503.07237 [hep-lat]].

[25] H. Na *et al.* [HPQCD Collaboration], Phys. Rev. D **92** (2015) no.5, 054510 Erratum: [Phys. Rev. D **93** (2016) no.11, 119906] doi:10.1103/PhysRevD.93.119906, 10.1103/PhysRevD.92.054510 [arXiv:1505.03925 [hep-lat]].

[26] C. McNeile, C. T. H. Davies, E. Follana, K. Hornbostel and G. P. Lepage, Phys. Rev. D **86** (2012) 074503 doi:10.1103/PhysRevD.86.074503 [arXiv:1207.0994 [hep-lat]].

[27] J. A. Bailey *et al.* [Fermilab Lattice and MILC Collaborations], Phys. Rev. D **89** (2014) no.11, 114504 doi:10.1103/PhysRevD.89.114504 [arXiv:1403.0635 [hep-lat]].

[28] C. Bernard *et al.*, Phys. Rev. D **79** (2009) 014506 doi:10.1103/PhysRevD.79.014506 [arXiv:0808.2519 [hep-lat]].

[29] S. Hashimoto, A. S. Kronfeld, P. B. Mackenzie, S. M. Ryan and J. N. Simone, Phys. Rev. D **66** (2002) 014503 doi:10.1103/PhysRevD.66.014503 [hep-ph/0110253].

[30] S. Hashimoto, A. X. El-Khadra, A. S. Kronfeld, P. B. Mackenzie, S. M. Ryan and J. N. Simone, Phys. Rev. D **61** (1999) 014502 doi:10.1103/PhysRevD.61.014502 [hep-ph/9906376].

[31] J. Harrison *et al.* [HPQCD Collaboration], Phys. Rev. D **97** (2018) no.5, 054502 doi:10.1103/PhysRevD.97.054502 [arXiv:1711.11013 [hep-lat]].

[32] A. Vaquero Avilés-Casco, C. DeTar, D. Du, A. El-Khadra, A. S. Kronfeld, J. Laiho and R. S. Van de Water, EPJ Web Conf. **175** (2018) 13003 doi:10.1051/epjconf/201817513003 [arXiv:1710.09817].

[33] A. V. Avilés-Casco *et al.* [Fermilab Lattice and MILC Collaborations], arXiv:1912.05886 [hep-lat].

[34] A. Vaquero, C. DeTar, A. X. El-Khadra, A. S. Kronfeld, J. Laiho and R. S. Van de Water, arXiv:1906.01019 [hep-lat].

[35] A. Vaquero talk presented at Lattice 2019, https://indico.cern.ch/event/764552/contributions/3421210/attachments/1863160/3062762/Lat19-Talk.pdf

[36] T. Kaneko *et al.* [JLQCD Collaboration], PoS LATTICE **2018** (2018) 311 doi:10.22323/1.334.0311 [arXiv:1811.00794 [hep-lat]].

[37] T. Kaneko *et al.* [JLQCD Collaboration], arXiv:1912.11770 [hep-lat].

[38] J. A. Bailey *et al.* [LANL-SWME Collaboration], EPJ Web Conf. **175** (2018) 13012 doi:10.1051/epjconf/201817513012 [arXiv:1711.01786 [hep-lat]].

[39] T. Bhattacharya *et al.* [LANL/SWME Collaboration], PoS LATTICE **2018** (2018) 283 doi:10.22323/1.334.0283 [arXiv:1812.07675 [hep-lat]].

[40] T. Bhattacharya *et al.* [LANL/SWME Collaboration], PoS LATTICE **2019** (2019) 056 [arXiv:2003.09206 [hep-lat]].

[41] M. B. Oktay and A. S. Kronfeld, Phys. Rev. D **78** (2008) 014504 doi:10.1103/PhysRevD.78.014504 [arXiv:0803.0523 [hep-lat]].

[42] J. A. Bailey, C. DeTar, Y. C. Jang, A. S. Kronfeld, W. Lee and M. B. Oktay, Eur. Phys. J. C **77** (2017) no.11, 768 doi:10.1140/epjc/s10052-017-5266-y [arXiv:1701.00345 [hep-lat]].

[43] J. A. Bailey *et al.* [LANL-SWME Collaboration], arXiv:2001.05590 [hep-lat].

[44] J. Flynn, R. Hill, A. JÃijttner, A. Soni, J. T. Tsang and O. Witzel, arXiv:1912.09946 [hep-lat].

[45] E. McLean, C. T. H. Davies, A. T. Lytle and J. Koponen, Phys. Rev. D **99** (2019) no.11, 114512 doi:10.1103/PhysRevD.99.114512 [arXiv:1904.02046 [hep-lat]].

[46] J. A. Bailey *et al.*, Phys. Rev. D **85** (2012) 114502 Erratum: [Phys. Rev. D **86** (2012) 039904] doi:10.1103/PhysRevD.85.114502, 10.1103/PhysRevD.86.039904 [arXiv:1202.6346 [hep-lat]].

[47] A. Bazavov *et al.* [Fermilab Lattice and MILC Collaborations], Phys. Rev. D **100** (2019) no.3, 034501 doi:10.1103/PhysRevD.100.034501 [arXiv:1901.02561 [hep-lat]].

[48] M. Atoui, V. Morénas, D. Becirevic and F. Sanfilippo, Eur. Phys. J. C **74** (2014) no.5, 2861 doi:10.1140/epjc/s10052-014-2861-z [arXiv:1310.5238 [hep-lat]].

[49] J. Flynn *et al.*, PoS LATTICE **2016** (2016) 296 doi:10.22323/1.256.0296 [arXiv:1612.05112].

[50] J. M. Flynn, R. C. Hill, A. Jüttner, A. Soni, J. T. Tsang and O. Witzel, PoS LATTICE **2018** (2019) 290 doi:10.22323/1.334.0290 [arXiv:1903.02100 [hep-lat]].

[51] E. McLean, C. T. H. Davies, J. Koponen and A. T. Lytle, arXiv:1906.00701 [hep-lat].

[52] C. J. Monahan, H. Na, C. M. Bouchard, G. P. Lepage and J. Shigemitsu, Phys. Rev. D **95** (2017) no.11, 114506 doi:10.1103/PhysRevD.95.114506 [arXiv:1703.09728 [hep-lat]].

[53] A. Abdesselam *et al.* [Belle Collaboration], arXiv:1904.08794 [hep-ex].

[54] P. Boyle, F. Erben, M. Marshall, F. Ó. hÓgáin, A. Portelli and J. T. Tsang, arXiv:1912.07563 [hep-lat].

[55] J. Harrison, C. Davies, A. Lytle, PoS BEAUTY **2019** (2019) 059.

[56] A. Lytle, B. Colquhoun, C. Davies, J. Koponen and C. McNeile, PoS BEAUTY **2016** (2016) 069 doi:10.22323/1.273.0069 [arXiv:1605.05645 [hep-lat]].

[57] B. Colquhoun *et al.* [HPQCD Collaboration], PoS LATTICE **2016** (2016) 281 doi:10.22323/1.256.0281 [arXiv:1611.01987 [hep-lat]].